BIOCHEMISTRY
including biophysical chemistry & molecular biology

Article

pubs.acs.org/biochemistry

Revealing the Allosterome: Systematic Identification of Metabolite–Protein Interactions

Thomas Orsak,[†] Tammy L. Smith,[†] Debbie Eckert,[†] Janet E. Lindsley,[†] Chad R. Borges,[‡,§] and Jared Rutter*[,†]

[†]Department of Biochemistry, University of Utah School of Medicine, Salt Lake City, Utah 84132, United States

[‡]Department of Pharmacology and Toxicology, University of Utah, Salt Lake City, Utah 84112, United States

Supporting Information

ABSTRACT: Small molecule allostery modifies protein function but is not easily discovered. We introduce mass spectrometry integrated with equilibrium dialysis for the discovery of allostery systematically (MIDAS), a method for identifying physiologically relevant, low-affinity metabolite–protein interactions using unmodified proteins and complex mixtures of unmodified metabolites. In a pilot experiment using five proteins, we identified 16 known and 13 novel interactions. The known interactions included substrates, products, intermediates, and allosteric regulators of their protein partners. MIDAS does not depend upon enzymatic measurements, but most of the new interactions affect the enzymatic activity of the protein partner. We found that the fatty acid palmitate interacts with both glucokinase and glycogen phosphorylase. Further characterization revealed that palmitate inhibited both enzymes, possibly providing a mechanism for sparing carbohydrate catabolism when fatty acids are abundant.

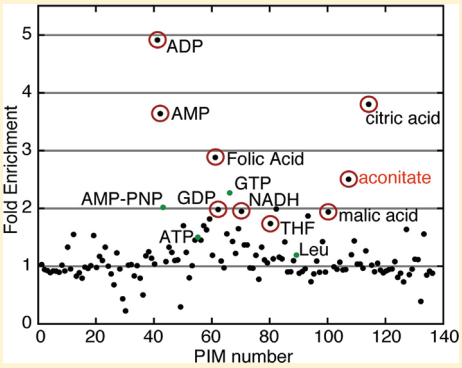

Virtually every complex cellular activity requires proper control of protein abundance, localization, and activity. Protein regulation occurs through a variety of mechanisms, including alteration of transcription, dynamic posttranslational modifications, and noncovalent interaction with small molecule metabolites or small molecule allostery (we will use the term allostery to specifically refer to small molecule allostery). Allosteric regulation involves a change in protein conformation, which modifies the localization, stability, interactions, or enzymatic activity of the protein. Through allosteric regulation, a protein can instantaneously respond to the metabolic landscape, allowing the cell to adapt in a rapidly changing environment.

Even more than transcriptional and post-translational regulation, identifying new allosteric regulators can be extremely difficult for a number of reasons.[1] Allosteric discoveries made to date have been made almost exclusively using assays of the protein's enzymatic activity. While this methodology has led to incredibly important observations, it is not useful for discovery of interactions that do not change an in vitro measurable activity. To allow discovery of these interactions in vitro, one needs a method that relies on measuring binding rather than protein activity. This raises the second major challenge of discovering allosteric regulators. For allosteric regulation to be dynamic and responsive to physiologically relevant changes, the affinity (dissociation constant or K_d) of the metabolite for the protein must be in or near the range of the metabolite concentration. For many important allosteric regulators, like ATP and glucose 6-phosphate, this concentration is in the high micromolar to low millimolar range. Therefore, we would expect the K_d for these interactions to be in a similar range. Such weak interactions are hard to study and harder to discover using conventional interaction methodologies.[1−4] Finally, most methods for the discovery of small molecule binding require immobilization or modification of one of the two molecules,[2,4,5] which can destroy or alter some interactions. As a result, the rate of discovery of small molecule allostery has been overwhelmingly outpaced by discoveries of transcriptional regulation or post-translational modification. However, in the past, when it was typical to screen for allosteric regulation of metabolic enzymes, it was found regularly.[1] It is logical to assume that it would similarly be found for the vast throng of more newly discovered and characterized proteins. What has been missing, however, is a method for systematically identifying these interactions that does not depend on a measurement of protein activity.

MATERIALS AND METHODS

Supplies. Glutamate dehydrogenase was purchased from Sigma (product G7882). $NADP^+$ specific glucose-6-phosphate dehydrogenase was purchased from Sigma (product G4134). Phosphoglucomutase and non-$NADP^+$ specific glucose-6-phosphate dehydrogenase were purchased from Roche. Phosphofructokinase was a gift from K. Uyeda. Glucokinase

Received: August 19, 2011
Revised: November 8, 2011
Published: November 28, 2011

was a gift from T. Saeki. All other compounds were purchased from Sigma.

Equilibrium Dialysis and Sample Preparation. Dialysis was conducted for 4 h at 4 °C in 0.5 mM protein-containing chambers separated by an equilibrium dialysis membrane from a large reservoir of compounds at 10 μM each; 25 μL of equilibrated sample solution was collected from each of four protein- and non-protein-containing chambers and from the large reservoir. To each sample was added 200 μL of ice-cold MeOH, and the mixture was incubated at −20 °C for 1 h to precipitate the protein. Proteins were then pelleted by centrifugation for 20 min at 4 °C. The supernatant was collected and either stored at −80 °C for GC samples or further cleared of protein by being spun through a Micron YM-3 device (product 42404) at 14000 RCF for 4 h and then stored at −80 °C.

GC−MS Sample Handling. Samples from equilibrium dialysis experiments or stock solutions containing a mixture of all analytes (n = 5 at 5 μM and n = 5 at 10 μM per batch) were placed in silanized 13 mm × 100 mm round-bottom glass test tubes and dried at 40 °C under a gentle stream of air. To these samples was added 1.5 μL of dimethylformamide (DMF) followed by vortexing and then 50 μL of MSTFA followed by additional vortexing. (Addition of DMF dramatically improves the recovery and quantitative precision of a number of analytes, particularly sugars. Too much DMF, however, will lead to chromatographic fronting.) Samples were heated at 75 °C for 25 min and then transferred to autosampler vials.

Analysis of samples by GC−MS was conducted on an Agilent GC-MSD instrument consisting of an Agilent 6890 gas chromatograph coupled to an Agilent 5973 Inert mass spectrometer (G2579A Performance turbo EI MSD model). Samples (1 μL) were injected in split mode (2:1) onto a split/splitless injector kept at 280 °C. The gas chromatograph was operated in constant flow mode with an average carrier gas (He) linear velocity of 35 cm/s through a DB-1MS, 30 m × 0.25 mm (inside diameter), 0.1 μm film capillary column. The initial oven temperature was set to 80 °C and without any initial hold time was increased at a rate of 10 °C/min to 255 °C, followed by an increase at a rate of 30 °C/min to 320 °C and a final hold for 2.1 min. The GC−MS transfer line was kept at 325 °C. The ion source was operated in EI mode at 230 °C, with a 70 eV filament. The quadrupole was operated at 150 °C in SIM mode, yielding data for three or four ions of interest per analyte. Following data acquisition, target ion-extracted ion chromatogram peak areas for analytes were obtained via automated integration and directly used as a relative measure of analyte concentration.

LC−MS Sample Handling. The LC−MS equipment consisted of an Agilent 1100 series high-performance liquid chromatography system with an in-line degasser, a column heater, and an autosampler equipped with a 100 μL injection loop connected to an Applied Biosystems QStar-XL tandem mass spectrometer equipped with a Turboionspray (heated electrospray) ion source. Five microliter loop injections were made. In positive mode, the mobile phase consisted of 0.1% (v/v) formic acid in water (25%) and methanol (75%). In negative mode, the mobile phase consisted of 20% ultrapure water and 80% methanol. The mobile phase was pumped at a flow rate of 250 μL/min. Single injections (runs) lasted for 1 min each.

In both polarity modes, the mass spectrometer was operated in TOF MS mode with an m/z range of 70−1500 Th under the following conditions. The ESI probe position was 5 mm off axis to the left and 1.5 mm back from the closest possible setting. The nebulizer gas (gas 1) was set at 60 arbitrary units, the auxiliary gas (gas 2 or heated gas) at 80 arbitrary units, the curtain gas at 45 arbitrary units, the auxiliary gas temperature at 400 °C, and the ESI voltage at 4000 V (−4000 V for negative ion mode).

GC−MS and LC−MS Validation Methods. The purpose of the analytical methods employed was to detect a statistically significant increase in instrument response (i.e., chromatographic peak area) upon analysis of a sample containing an analyte at a concentration 2-fold greater than that in equilibrium dialysis dialysates. To model the way in which proteins were to be screened for allosteric modulators, we included all analytes in every sample for a given analytical set (GC−MS, LC−MS positive, or LC−MS negative mode set). For the GC−MS set of compounds, two sets [n = 10 aliquots (25 μL) each] of sample concentrations, one at 10 μM and one at 20 μM, were employed. For the LC−MS sets, which are diluted following ED, four sample concentrations (n = 5 diluted 25 μL aliquots each at 200 nM, 400 nM, 2 μM, and 4 μM) were tested. With regard to LC−MS in particular, signal increases for individual analytes should be less intense if all analytes are validated (i.e., increased in concentration) simultaneously than if individual analytes were to be validated one at a time.

Protein Purification of Yeast Glycogen Phosphorylase. N- or C-terminally His_6-tagged yGPH was produced in BL21 *Escherichia coli* cells transformed with yGPH-expressing pHis-Parallel vector. When cells reached an absorbance of 0.6 at 600 nm, yGPH production was induced by 1 mM IPTG and cells were allowed to produce protein for 16 h at 25 °C. yGPH was purified first by using Ni-NTA agarose (Qiagen) to bind the His_6 tag and then by fast-performance liquid chromatography (FPLC) using a MonoQ 5/50 GL column (Amersham).

Phosphorylation of Yeast Glycogen Phosphorylase. yGPH was phosphorylated by bovine cAMP-dependent protein kinase catalytic subunit (Sigma) at a 400:1 (w/w) ratio of yGPH to kinase. The reaction was performed in 50 mM Tris (pH 7.5) with 2 mM DTT, 10 mM $MgCl_2$, and 1 mM ATP at 25 °C for 5 h. yGPH-P was purified from yGPH by FPLC using a MonoQ 5/50 GL column and a Superdex 200 10/300 GL column (Amersham).

Yeast Glycogen Phosphorylase Kinetic Assay. Steady state kinetics for phosphorylated or nonphosphorylated yGPH were determined in the direction of glucose 1-phosphate synthesis using a phosphoglucomutase (converts glucose 1-phospate to glucose 6-phosphate) and glucose-6-phosphate dehydrogenase (converts $NADP^+$ to NADPH and glucose 6-phosphate to 6-phosphoglucono-δ-lactone) coupled reaction. The reaction was performed in 50 mM Tris-HCl (pH 7.4), 10 mM DTT, 0.2 mM $NADP^+$, 0.1 mM glucose 1,6-diphosphate, varied glycogen concentrations, 2 units/mL glucose-6-phosphate dehydrogenase, 1.2 units/mL phosphoglucomutase, and varied inorganic phosphate concentrations (using a diluted 1000 mM KH_2PO_4/100 mM Na_2HPO_4 mixture) at 25 °C. Absorbance was measured every 30 s at 340 nm on an Optima 96-well spectrometer to detect NADPH production. The initial linear range of the absorbance increase over time was used to calculate the yGPH reaction rate.

NAD Kinase Kinetic Assay. Steady state kinetics for NADK were determined in the direction of $NADP^+$ synthesis using a $NADP^+$ specific glucose-6-phosphate dehydrogenase (converts $NADP^+$ to NADPH and glucose 6-phosphate to 6-phosphoglucono-δ-lactone) coupled reaction. The reaction was

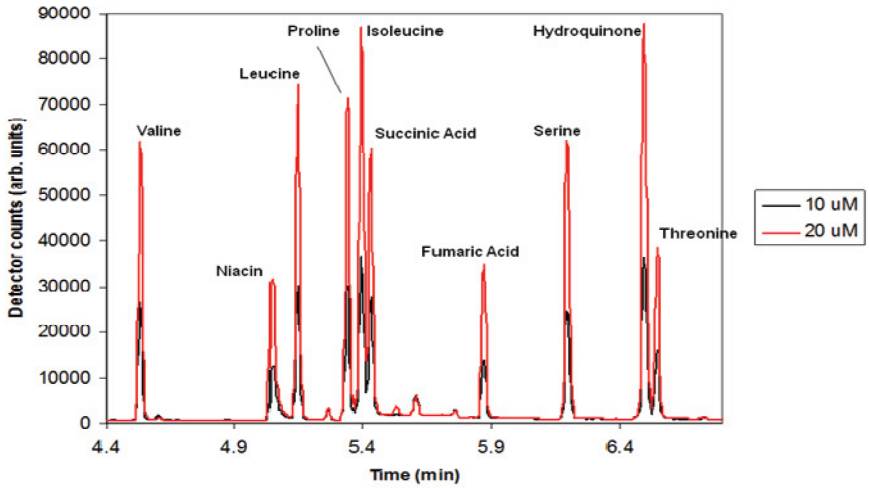

Figure 1. Illustrative precision control GC–MS data. Shown are sections of the total ion current chromatograms (TICs) for two mixtures of PIMs, one at 10 μM and the other at 20 μM. The data demonstrate the doubling of the instrumental response upon doubling of the PIM concentration. A few PIMs overlap chromatographically at the TIC level but are completely separate when viewed as extracted ion chromatograms that are actually employed for chromatographic peak area integration and determination of PIM abundance.

Chart 1. Representative Analytical Method Validation Data for 22 of the PIMs To Be Analyzed by GC–MS[a]

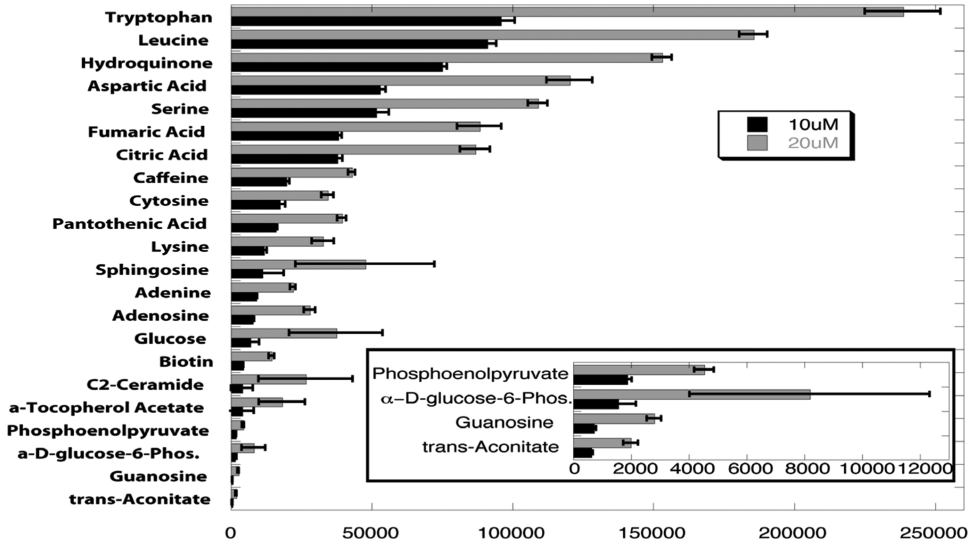

[a]Aliquots (25 μL) of two mixtures of PIMs, one mixture containing each PIM at 10 μM (n = 29) and the other mixture containing each PIM at 20 μM (n = 10), were dried under a gentle stream of air and then derivatized and analyzed by GC–MS as described above. Extracted ion chromatogram peak areas for a specific "target ion" for each PIM were used for quantification. Average values are shown. Please note that the error bars are ± two standard deviations. Therefore, we can easily detect a 2-fold enrichment for almost all compounds even employing a stringent two-standard deviation cutoff.

performed in 100 mM Tris-HCl (pH 7.4), 10 mM MgCl, varied (10 mM) NAD^+ concentrations, varied ATP concentrations, 3 mM glucose 6-phosphate, and 5 units/mL glucose-6-phosphate dehydrogenase (Sigma, product G4134) at 25 °C. Absorbance was measured every 30 s at 340 nm on an Optima 96-well spectrometer. The initial linear range of the absorbance increase over time was used to calculate the NADK reaction rate.

Glutamate Dehydrogenase Kinetic Assay. Steady state kinetics for glutamate dehydrogenase were determined in the NADPH synthesis direction. The reaction was performed in 100 mM Tris-HCl (pH 7.4), varied $NADP^+$ concentrations, and varied glutamate concentrations at 25 °C. Absorbance was measured every second at 340 nm on an Ultraspec2100 spectrometer. The initial linear range of the absorbance increase over time was used to calculate the glutamate dehydrogenase reaction rate.

Glucokinase Kinetic Assay. Steady state kinetics for glucokinase were determined in the glucose 6-phosphate synthesis direction using a glucose-6-phosphate dehydrogenase (converts $NADP^+$ to NADPH and glucose 6-phosphate to 6-phosphoglucono-δ-lactone) coupled reaction. The reaction was performed in 50 mM HEPES (pH 8.0), 3 mM MgCl, 1 mM $NADP^+$, 25 mM KCl, 2 mM DTT, 0.002 unit/μL glucose-6-phosphate dehydrogenase, varied ATP concentrations, and varied glucose concentrations. Absorbance was measured every 30 s at 340 nm on an Optima 96-well spectrometer. The initial

dx.doi.org/10.1021/bi201313s | *Biochemistry* 2012, 51, 225–232

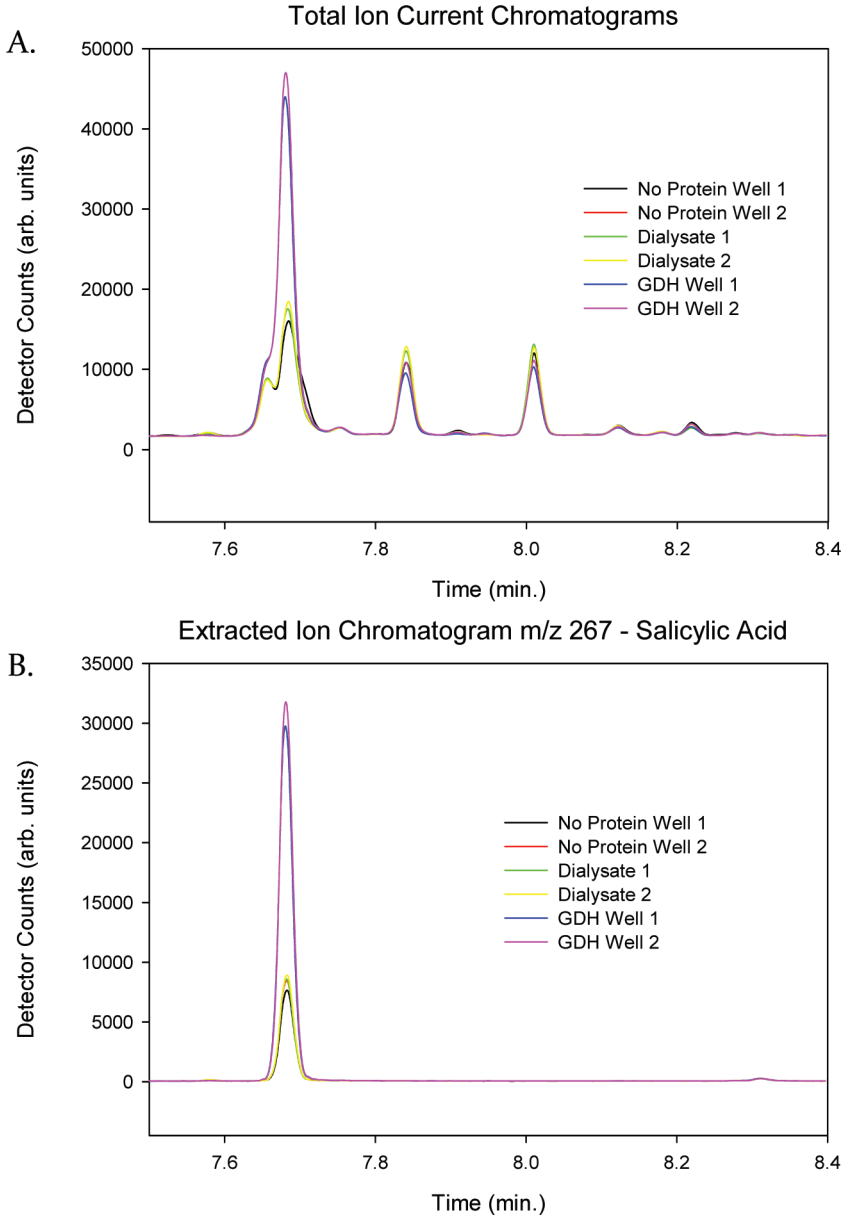

Figure 2. Illustrative protein sample GC–MS data. Shown are sections of the ion chromatograms for GDH protein samples equilibrated with the GC PIM solution with controls. (A) Total ion current chromatogram (TIC) for GDH. The data demonstrate the increased instrumental response of enriched and nonenriched PIMs in the GDH-containing wells (GDH Well) over wells with no protein (No Protein Well) and PIM dialysate outside of the wells (Dialysate). A few PIMs overlap chromatographically at the TIC level but (B) are completely separate when viewed as extracted ion chromatograms. Both malate and salicylic acid are enriched and overlap in the TIC (A) but can be separated as shown with salicylic acid in the extracted ion chromatogram (B).

linear range of the absorbance increase over time was used to calculate the Glucokinase reaction rate.

Ultracentrifugation. Purified yGPH-P was dialyzed with Tris-HCl (pH 7.5) and then diluted to absorbance values of 0.5, 0.25, and 0.125 at 280 nm in Tris-HCl (pH 7.5) with or without compounds of interest. The solutions were then centrifuged at four speeds for a total of 48 h in a Beckman Optima XL-A analytical ultracentrifuge, and molecular weight fits and K_a values were determined using sedimentation equilibrium analysis by HeteroAnalysis, downloaded from http://www.biotech.uconn.edu/auf/?i=aufftp.

RESULTS

Herein, we describe mass spectrometry integrated with equilibrium dialysis for the discovery of allostery systematically (MIDAS), a method capable of rapidly identifying metabolite interactors for unmodified soluble proteins out of a complex mixture of unmodified putative interacting metabolites (PIMs). The initial step involves equilibrium dialysis of the purified protein at a high concentration against a mixture of biologically relevant small molecules. Briefly, a small volume of the purified protein is separated by a semipermeable membrane from a relatively large volume containing a complex mixture of metabolites (Figure 1 of the Supporting Information). Each PIM reaches equilibrium across the membrane with the same free concentration in both compartments. The total concen-

dx.doi.org/10.1021/bi201313s | *Biochemistry* 2012, 51, 225–232

tration (including free and protein-bound) of the metabolite is elevated, however, within any chamber containing a protein with which it interacts. Finally, the relative concentration of each metabolite in both protein-containing chambers and empty control chambers is quantified using liquid or gas chromatography-coupled mass spectrometry (LC−MS or GC−MS, respectively).

For reliable quantification by mass spectrometry, the 138 PIMs in our test were divided into three mixtures designed for GC−MS or LC−MS in either the positive or negative mode (Table 1 of the Supporting Information). The 138 metabolites include proteinogenic amino acids, major carbohydrates, various phospho forms of the major nucleotides, major cofactors, and coenzymes, known signaling molecules, and intermediates in glycolysis, lipid metabolism, and the TCA cycle. The concentration of each PIM in the respective mixture was 10 μM. Before protein interaction analysis, we validated our MS analytical methodology to ensure we could minimally detect all interactions with a K_d of ~500 μM. For this validation, we analyzed the mixtures at 10 and 20 μM. Illustrative GC−MS data are provided in Figure 1. The peak area quantitation for a subset of PIMs (± two standard deviations) is shown in Chart 1. We concluded that our quantitation methods allow us to detect a 2-fold increase in PIM concentration with 99.9% confidence. Therefore, we believed that we should be able to detect interactions with substantially weaker affinity than the ~500 μM threshold, albeit with slightly less confidence. In addition, we ran a precision control set with each batch of samples described below. Each precision control set duplicated the validation sets just described. Thus, we are able to have confidence that PIM responses from unknown samples are valid and robust.

Using the validated analytical methods, we performed the complete procedure, beginning with dialysis of 50 μL of each purified protein at 0.5 mM with the PIM mixtures (see Figure 1 of the Supporting Information for the equilibrium dialysis apparatus). The proteins were highly purified *Salmonella typhimurium* NAD kinase (styNADK), *Saccharomyces cerevisiae* glycogen phosphorylase (yGPH), human glucokinase (hGK), L-glutamate dehydrogenase type III from bovine liver (GDH), and *E. coli* phosphofructokinase (PFK). The PIMs were allowed to equilibrate with the protein-containing compartment; the equilibrated protein/metabolite solutions were collected, and the proteins were denatured, precipitated, and cleared from the metabolite solution. Relative PIM concentrations were determined by GC−MS or LC−MS. Hits were defined as being enriched in the protein-containing wells over control wells to two standard deviations (see Figure 2 for GDH GC−MS chromatograms). In total, for the five proteins analyzed, we detected 16 previously reported and 13 previously undescribed interactions (Table 1). The 16 known interactions encompass many of the known allosteric regulators, substrates, and products for the five proteins tested. In addition, we attempted to test the 13 novel interactions identified by MIDAS for effects on protein catalytic activity using in vitro enzymatic assays.

NAD kinase catalyzes the conversion of NAD^+ to $NADP^+$ using ATP as the phosphate donor. We identified four known and seven unreported interactions for this protein. We detected the two products of catalysis, ADP and $NADP^+$, and allosteric inhibitors NADH and NADPH.[6] The unreported interacting molecules include other adenine nucleotides, AMP, and diadenosine pentaphosphate; three coenzymes structurally similar to adenine nucleotides, coenzyme A, folic acid, and pyridoxal phosphate; and two seemingly unrelated metabolites, aminolevulinic acid and glucose 6-phosphate (Table 1).

Table 1. Interactors Identified by MIDAS[a]

Previously Reported Interaction			Function	
styNADK	ADP		product	
DK	NADH		inhibitor	
	$NADP^+$		product	
	NADPH		inhibitor	
yGPH	glucose 6-phosphate		inhibitor	
hGK	ADP		product	
	pyridoxal phosphate		inhibitor	
GDH	ADP		activator	
	AMP		interactor	
	folic acid		inhibitor	
	GDP		activator	
	malic acid		inhibitor	
	NADH		substrate	
	salicylic acid		inhibitor	
	tetrahydrofolic acid		inhibitor	
PFK	fructose 6-phosphate		substrate	
novel interaction		**allostery substrate**	**K_i or K_o**	**standard error**
styNADK	aminolevulinic acid	NC		
	AMP	un-ATP	3.22	0.66
		un-NAD^+	5	1.11
	coenzyme A	NT		
	diadenosine pentaphosphate	non-ATP	4.9	0.51
		non-NAD^+	5.49	1.55
	folic acid	NT		
	glucose 6-phosphate	act-ATP	0.5 (K_o)	
		NC-NAD^+		
	pyridoxal phosphate	NT		
yGPH-P	fructose 6-phosphate	NT		
	guanosine	non-P_i	7.95	1.25
		un-glycogen	5.62	0.56
	palmitic acid	un-P_i	0.29	0.06
		com-glycogen	0.05	0.01
hGK	guanosine	NC		
	palmitic acid	com-ATP	0.14	0.05
		non(P)-glucose	0.01	0.01
HK	palmitic acid	NC		
GDH	*trans*-aconitate	un-NADP	2.31	0.42
		un-glutamate	2.16	0.46
	trans-aconitate and 4 mM leucine	com-glutamate	0.26	0.11

[a]Abbreviations: act, activator; com, competitive; NC, no change; non, noncompetitive; NT, not tested; P, partial; un, uncompetitive. Values are in millimolar.

Glycogen phosphorylase catalyzes the removal of one glucose moiety from the nonreducing end of glycogen. Phosphorolysis of the terminal glycosidic linkage produces glucose 1-phosphate using inorganic phosphate as the phosphate donor. We detected the only known allosteric regulator of yeast glycogen phosphorylase, glucose 6-phosphate, as well as three additional interactors, guanosine, palmitate, and the glucose 6-phosphate isomer, fructose 6-phosphate (Table 1).

Phosphofructokinase phosphorylates fructose 6-phosphate to fructose 1,6-bisphosphate using ATP as the phosphate donor.

dx.doi.org/10.1021/bi201313s | *Biochemistry* 2012, 51, 225−232

We identified only one interactor for PFK, the substrate fructose 6-phosphate (Table 1).

Glucokinase uses ATP to phosphorylate glucose to glucose 6-phosphate, releasing ADP, which was identified as an interactor along with the known inhibitor, pyridoxal phosphate. Two novel interactors were also observed: guanosine and palmitate.

Glutamate dehydrogenase catalyzes the conversion of glutamate to α-ketoglutarate and ammonia using water as an oxygen donor and NAD^+ or $NADP^+$ as an electron acceptor. Eight known interactions and one previously unknown interaction were identified for GDH, as seen circled in red in Figure 3. Four known interactions were not detected to the

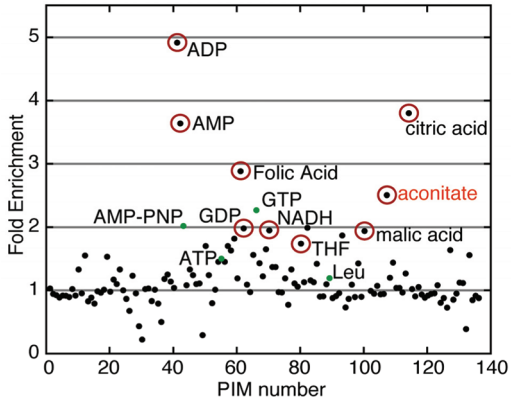

Figure 3. Metabolite analysis of glutamate dehydrogenase (GDH). Fold enrichment in the presence and absence of GDH plotted for each of the 138 PIMs. Compounds that are significantly (two standard deviations) different from the control are circled in red. Known GDH interactors that were not significantly enriched are denoted in green. A novel interactor, aconitate, identified by MIDAS is shown with red text.

required stringency level, although each was enriched in the protein-containing chamber (green dots). The eight previously reported interacting metabolites in our analysis were ADP, AMP, folic acid, GDP, malic acid, NADH, salicylic acid, and tetrahydrofolic acid. The one unreported interacting partner found, *trans*-aconitate, is similar to the product α-ketoglutarate.

We attempted to test the 13 novel interactions identified by MIDAS for effects on protein catalytic activity using in vitro enzymatic assays. Four of the 13 could not be assayed because of conflicts with the enzyme assay method; typically, the molecule inhibits one of the enzymes of the coupled assay system. Incidentally, the inhibition of the enzyme in the coupled assay system was not previously described. For example, glucose-6-phosphate dehydrogenase was inhibited by coenzyme A, folic acid, and pyridoxal phosphate, and either pyruvate kinase or lactate dehydrogenase is inhibited by guanosine and palmitic acid. As shown in Table 1, of the nine novel interactors that could be assayed, six were found to be inhibitors with an inhibition constant (K_i) in the low micromolar to low millimolar range, one is an activator, and two had no effect on in vitro enzymatic activity (in addition, a noninteracting control between hexokinase and palmitate is also shown to illustrate the specificity of the yGPH-P–palmitate interaction).

Seven unreported interactions were identified for styNADH. The variety of molecules that bound styNADK was surprising, but this may be true because of the central role that nicotinamide nucleotides play in metabolism. The NAD^+/NADH redox couple is a key energy currency in central metabolism. Further, NADPH is a required source of reducing equivalents for biosynthetic processes, including lipid biosynthesis, and for detoxification of oxidative species. The only activator found in this study was glucose 6-phosphate activation of styNADK; 20 mM glucose 6-phosphate shifts styNADK's K_m for ATP from 2 to 0.5 mM without effecting the K_m for NAD^+. Taken together, high levels of the styNADH inhibitors could represent a lower-energy state in the cell, implying weaker demand for $NADP^+$ or NADPH for biogenesis, while high levels of the activator, glucose 6-phosphate, could represent a state of adequate carbohydrate and sufficient energy for biogenesis and growth.

The structural similarities between a novel interactor of GDH, *trans*-aconitate, and the known inhibitor, α-ketoglutarate, led us to further characterize the regulation of GDH by *trans*-aconitate. α-Ketoglutarate inhibits GDH noncompetitively with glutamate in the absence of leucine and competitively with glutamate in the presence of leucine.[7] As shown in Table 1, *trans*-aconitate inhibits GDH and the inhibitory mode also changes in the presence of leucine, from uncompetitive to competitive. This suggests that *trans*-aconitate is inhibiting GDH in a manner similar to that of α-ketoglutarate and may play an inhibitory role similar to that of GDH in vivo. Additionally, *trans*-aconitate is a known inhibitor of aconitase[8,9] and fumarase[10] in the citric acid cycle and is produced enzymatically or spontaneously[11] from the citric acid cycle intermediate, *cis*-aconitate. Therefore, GDH inhibition may be another way *trans*-aconitate can signal to slow production of citric acid cycle intermediates.

We found two novel interactions for glucokinase, guanosine and palmitate. As both molecules directly affected the pyruvate kinase/lactate dehydrogenase coupled assay system, we turned to an assay of glucose 6-phosphate. We observed no change in the activity of hGK in the presence of guanosine but saw strong inhibition by palmitate. We were concerned that this might be due to a nonspecific detergent-like effect of palmitate on hGK. If that were true, we would expect that palmitate would have similar effects on the highly similar hexokinase (HK) enzyme. Under conditions that were identical to those of the glucokinase experiments, palmitate had no effect on HK enzymatic activity (Table 1). Furthermore, palmitoyl-CoA has been previously shown to inhibit hGK.[12] These data argue against a nonspecific effect on the protein structure or active site. In hepatocytes, the inhibition of the rate-limiting step of glycolysis, glucose phosphorylation and retention, through inhibition of glucokinase is a logical physiological response to elevated fatty acid concentrations. In this way, the cell can utilize the excess fatty acid, which could be toxic if left unused or unesterified, as a fuel source and spare circulating glucose for glucose-dependent tissues like the brain. Indeed, this effect has been observed physiologically in primary rat hepatocytes.[13] It is tempting to speculate that a portion of this effect is mediated by fatty acid allosteric inhibition of glucokinase.

We used the active phosphorylated form of yGPH (yGPH-P) to test for allosteric regulation by the novel interactors, fructose 6-phosphate, guanosine, and palmitic acid. We were unable to enzymatically test the effects of fructose 6-phosphate on yGPH-P because of the contamination of fructose 6-phosphate with glucose 6-phosphate, a known inhibitor of yGPH and the product and substrate, respectively, of the enzymes of our coupled assay system, phosphoglucomutase and glucose-6-

phosphate dehydrogenase. Palmitate was found to be the most potent inhibitor of yGPH-P, with a K_i of ~50 μM versus glycogen. As described above for glucokinase, the inhibition of glycogen mobilization in the presence of an alternate fuel source, such as fatty acids, is a logical physiological response. In this way, the cell can utilize the excess fatty acid and save its glycogen reserves for a potential future period of energetic challenge.

Other fatty acids, including stearic acid and lauric acid, also exhibited an ability to inhibit yGPH-P in a similar concentration range (data not shown), while palmitoleic acid was untestable because it inhibits one or both of the coupled enzymes, either glucose 6-phosphate and phosphoglucomutase. In addition, we observed that the quaternary state of C-terminally His_6-tagged yGPH was altered by palmitate. It is known that the GPH inhibitor glucose 6-phosphate causes a change in quaternary structure from a dimer to a tetramer, which is thought to be a component of the inhibitory activity. We were able to observe this same phenomenon using analytical ultracentrifugation of His_6-tagged yGPH using 10 mM glucose 6-phosphate (Table 2 of the Supporting Information). We observed an almost identical shift in quaternary state using only 0.2 mM palmitate. Concerned about potential detergent-like effects of the amphipathic palmitate, we determined whether identical concentrations of sodium dodecyl sulfate (SDS) similarly affected yGPH quaternary structure, but SDS had no effect (Table 2 of the Supporting Information).

Finally, to test whether palmitate inhibition of phosphorylase extends to higher organisms, we tested its effect on rabbit glycogen phosphorylase "active form" A and "inactive form" B. Similar concentrations of palmitate required to inhibit yGPH-P also inhibited phosphorylase A in the presence or absence of 50 mM glucose (Figure 2 of the Supporting Information). Phosphorylase B was also inhibited by similar concentrations of palmitate in the presence of 0.02 mM AMP, an activator of form B, but not in in the absence of AMP (data not shown).

DISCUSSION

We have demonstrated that the MIDAS methodology can effectively identify protein−small molecule interactions while avoiding many of the challenges that plague efforts to identify them. First, low- and high-affinity interactions were identified. Second, MIDAS does not require measurement of enzymatic activity. Third, complex mixtures of PIMs can be tested concurrently, making mid- to high-throughput analysis a possibility. Finally, proteins and small molecules do not need to be modified.

Challenges remain, however. First, MIDAS requires purified protein at high concentrations and consumes 50 μL per data point. This challenge could be somewhat mitigated by using a smaller dialysis format, such as a 96-, 384-, or 1496-plate format, which is well within the sensitivity of mass spectrometry analysis and would make the method compatible with powerful high-throughput analysis systems. Second, 138 metabolites is a massive underrepresentation of the biological complement. The powerful separation and analytical technology of mass spectrometry make it highly feasible to expand the analysis dramatically, pending only validation of the analytical method. Finally, we did not identify all known interactions in our mixtures for each protein. This is likely due to competition for binding sites by other molecules in the mixture and could be solved by subsequent experiments using mixtures lacking known interactors.

Identification of novel small molecule−protein interactions can lead to a more complete understanding of protein and cellular regulation and may help to identify enzymatic activities for proteins currently unassigned such functions, which comprise a majority of the proteins encoded by the human genome. This method may also be useful for the identification of regulatory sites accessible to small molecule drugs, as allosteric drugs are becoming a prized therapeutic approach.[14−16] In summary, MIDAS is a powerful approach with clear applications in improving our understanding of biological regulation, proteome annotation, and drug discovery.

ASSOCIATED CONTENT

Supporting Information

Supplemental data, including tables and figures referenced in the text. This material is available free of charge via the Internet at http://pubs.acs.org.

AUTHOR INFORMATION

Corresponding Author

*E-mail: rutter@biochem.utah.edu. Phone: (801) 581-3340.

Present Address

[§]Biodesign Institute, Arizona State University, Tempe, AZ 85287.

Funding

This work was supported by National Institutes of Health Grant DK071962 (J.R.) and by a Seed Grant from the University of Utah (J.R.).

ACKNOWLEDGMENTS

We thank Dr. Marty Rechsteiner and Dr. Michael Kay for the use of their equipment. We thank Julianne Grose and John Roth for the NADK protein, Ko Uyeda for PFK, and Don Blumenthal for glycogen phosphorylase.

REFERENCES

(1) Lindsley, J. E., and Rutter, J. (2006) Whence cometh the allosterome? *Proc. Natl. Acad. Sci. U.S.A. 103*, 10533−10535.

(2) Comess, K. M., Schurdak, M. E., Voorbach, M. J., Coen, M., Trumbull, J. D., Yang, H., Gao, L., Tang, H., Cheng, X., Lerner, C. G., McCall, J. O., Burns, D. J., and Beutel, B. A. (2006) An ultraefficient affinity-based high-throughout screening process: Application to bacterial cell wall biosynthesis enzyme MurF. *J. Biomol. Screening 11*, 743−754.

(3) Li, X., Gianoulis, T. A., Yip, K. Y., Gerstein, M., and Snyder, M. (2010) Extensive in vivo metabolite-protein interactions revealed by large-scale systematic analyses. *Cell 143*, 639−650.

(4) Vuignier, K., Schappler, J., Veuthey, J., Carrupt, P., and Martel, S. (2010) Drug-protein binding: A critical review of analytical tools. *Anal. Bioanal. Chem. 398*, 53−66.

(5) Vegas, A. H., Fuller, J. H., and Koehler, A. N. (2008) Small-molecule microarrays as tools in ligand discovery. *Chem. Soc. Rev. 37*, 1385−1394.

(6) Grose, J. H., Joss, L., Velick, S. F., and Roth, J. R. (2006) Evidence that feedback inhibition of NAD kinase controls responses to oxidative stress. *Proc. Natl. Acad. Sci. U.S.A. 103*, 7601−7606.

(7) Fahien, L. A., MacDonald, M. J., Kmiotek, E. H., Mertz, R. J., and Fahien, C. M. (1988) Regulation of insulin release by factors that also modify glutamate dehydrogenase. *J. Biol. Chem. 263*, 13610−13614.

(8) Saffran, M., and Prado, J. L. (1949) Inhibition of aconitase by trans-aconitate. *J. Biol. Chem. 180*, 1301−1309.

(9) Lauble, H., Kennedy, M. C., Beinert, H., and Stout, C. D. (1994) Crystal structures of aconitase with trans-aconitate and nitrocitrate bound. *J. Mol. Biol. 237*, 437−451.
(10) Rebholz, K. L., and Northrop, D. B. (1994) Kinetics of enzymes with iso-mechanisms: Dead-end inhibition of fumarase and carbonic anhydrase II. *Arch. Biochem. Biophys. 312*, 227−233.
(11) Ambler, J. A., and Roberts, E. J. (1948) The effect of pH on the stability of cis-aconitic acid in dilute solution. *J. Org. Chem. 13*, 399−408.
(12) Dawson, C. M., and Hales, C. N. (1969) The inhibition of rat liver glucokinase by palmitoyl-CoA. *Biochim. Biophys. Acta 179*, 657−659.
(13) Swagell, C. D., Morris, C. P., and Henly, D. C. (2006) Effect of fatty acids, glucose, and insulin on hepatic glucose uptake and glycolysis. *Nutrition 22*, 672−678.
(14) Christopoulos, A. (2002) Allosteric binding sites on cell-surface receptors: Novel targets for drug discovery. *Nat. Rev. Drug Discovery 1*, 198−210.
(15) Conn, P. J., Cristopoulos, A., and Lindsley, C. W. (2009) Allosteric modulators of GPCRs: A novel approach for the treatment of CNS disorders. *Nat. Rev. Drug Discovery 8*, 41−54.
(16) Shoichet, B. K. (2006) Screening in a spirit haunted world. *Drug Discovery Today 11*, 607−615.